

# Regiosymmetric Dibutyl-Substituted Poly(3,4-propylenedioxythiophene)s as Highly Electron-Rich Electroactive and Luminescent Polymers

Dean M. Welsh, Leroy J. Kloeppner, Luis Madrigal, Mauricio R. Pinto, Barry C. Thompson, Kirk S. Schanze, Khalil A. Abboud, David Powell, and John R. Reynolds\*

Department of Chemistry, Center for Macromolecular Science and Engineering, University of Florida, Gainesville, Florida 32611

Received November 21, 2001; Revised Manuscript Received May 23, 2002

**ABSTRACT:** We report the synthesis of the dibutyl derivative of poly(3,4-propylenedioxythiophene) as a regiosymmetric and soluble electroactive and photoluminescent conjugated polymer obtained in the neutral form by a Grignard metathesis coupling reaction. Molecular weights have been characterized by gel permeation chromatography (GPC) and matrix-assisted laser desorption/ionization time-of-flight (MALDI–TOF) mass spectrometry, the latter showing end groups due to H/H, H/Br, and Br/Br termini. Solution-cast films of PProDOT-Bu<sub>2</sub> are reddish-purple with a  $\lambda_{\text{max}}$  value of 544 nm as deposited (576 nm after electrochemical annealing) and an electronic band gap of 1.8 eV. In solution, the polymer displays a strong deep red photoluminescence, and transient absorption studies reveal that direct excitation also affords a long-lived triplet state with low-to-moderate quantum efficiency. The photoluminescence is considerably weaker in the solid state, presumably due to rapid nonradiative decay at interchain trap sites. The polymer is easily oxidized with an  $E_{1/2}$  of  $\sim 0.2$  V vs Ag/Ag<sup>+</sup> when prepared either by solution casting of the chemically synthesized polymer or by direct electrodeposition and provides a distinct electrochromic switch from a deep red-purple to a highly transmissive sky blue. Similar spectral changes are observed upon solution doping, and conducting films (up to 7 S/cm) have been prepared which exhibit a high level of ambient stability.

## Introduction

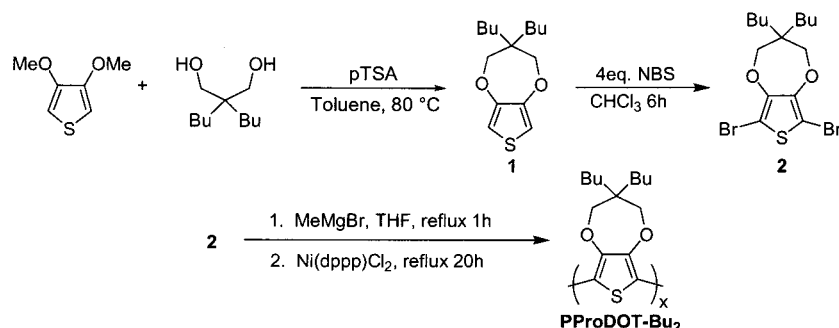
The development of soluble and processable highly conjugated and conducting polymers has opened up application possibilities that range from conductive anti-static coatings to polymer-based light-emitting devices.<sup>1</sup> Polythiophenes have been extensively investigated as one of the most important classes of conjugated polymers, where placing a sufficiently long alkyl group at the 3-position leads to solution and melt processable materials.<sup>2–5</sup> While facile oxidative polymerization methods lead to regiorregular polymers, these materials tend to have a low degree of order. The synthesis of structurally homogeneous, regioregular, head-to-tail poly(3-alkylthiophene)s (P3AT's), first by McCullough and co-workers<sup>6,7</sup> and subsequently by Rieke and co-workers,<sup>8,9</sup> yielded regular head-to-tail P3AT's with conductivity values that are 2 orders of magnitude greater than regiorandom polymers.<sup>10</sup>

Poly(3,4-ethylenedioxythiophene) (PEDOT) has attracted much attention over the past 10 years, and its chemistry has been recently reviewed.<sup>11</sup> PEDOT exhibits many favorable properties which include a reduced band gap, low oxidation potential for conversion to the conducting state, and high stability in the conducting form.<sup>12,13</sup> The ability of PEDOT to easily switch between an absorptive dark blue in its reduced form and a highly transmissive light blue in its oxidized form makes it useful as an electrochromic (EC) material. We have electrosynthesized a variety of structural derivatives of PEDOT that exhibit fast EC switching with high optical contrasts.<sup>14,15</sup> Of these derivatives, the fastest response times and greatest contrasts were obtained with a dimethyl-substituted 3,4-propylenedioxythiophene (PProDOT-Me<sub>2</sub>) polymer.<sup>16</sup> Along with PEDOT, these derivatives have been incorporated into dual-polymer electrochromic devices that exhibit high contrast in the visible and infrared regions with good long-term stability.<sup>17,18</sup>

Although electropolymerization is an invaluable technique in synthesizing conjugated polymers, it has limitations including lack of primary structure verification and the inability to form large amounts of processable polymer. Oxidative polymerization of alkyl<sup>19</sup> and alkoxy-substituted<sup>20</sup> EDOT, followed by chemical reduction of the as-produced oxidized polymer, leads to regiorandom-substituted PEDOTs that are soluble in common organic solvents. In general, it is difficult to fully reduce these easily oxidized polymers (charges are trapped on the conjugated chains), and it can be difficult to remove residual metal ion impurities when iron-based oxidants are used. Yamamoto et al. report on the direct synthesis of insoluble neutral PEDOT,<sup>21</sup> and soluble alkylated PEDOTs,<sup>22</sup> via Ni-promoted dehalogenation condensation where cyclic voltammetry and spectroelectrochemistry could be accomplished. As with the other derivatized PEDOTs, the lack of symmetry in the monomers lead to regiorregular and atactic polymers.

In this paper, we report the synthesis of the first soluble poly(3,4-alkylenedioxythiophene) polymer from a regiosymmetric monomer obtained in the neutral form by a transition-metal-catalyzed coupling reaction. Here we utilize the effective Grignard metathesis polymerization (GriM) method developed by McCullough et al.<sup>23,24</sup> which has been shown to yield high molecular weight (and regioregular) P3ATs and has been extended to EDOT derivatives in phenylene-linked hybrid copolymers.<sup>25</sup> The dialkylated 3,4-propylenedioxythiophene (ProDOT-R<sub>2</sub>) structure was chosen because of its regiosymmetry which necessarily yields regiosymmetric (no need for a regioregular polymerization) and isotactic polymer, along with its previously discussed favorable redox and electrochromic properties. Solubility allows for complete structural characterization, which was unobtainable in the electropolymerized PProDOT-R<sub>2</sub> derivatives.

Scheme 1



## Results and Discussion

**Synthesis.** As shown in Scheme 1, compound **1** (ProDOT-Bu<sub>2</sub>) was synthesized by a transesterification reaction between 3,4-dimethoxythiophene and 2,2-di-tert-butyl-1,3-propanediol. Methanol is removed from the reaction with a Soxhlet extractor filled with type 4A molecular sieves in order to drive the reaction to completion. Compound **1** was successfully brominated with addition of excess NBS to yield compound **2** as a viscous oil, which could be purified by column chromatography. Following the Grignard metathesis (Grim) procedure developed by McCullough and co-workers<sup>23</sup> for the preparation of regioregular poly(3-dodecylthiophene) and applied to EDOT containing polymers by Wang et al.,<sup>25</sup> compound **2** was treated with methylmagnesium bromide at reflux followed by addition of Ni(dppp)Cl<sub>2</sub> to yield PProDOT-Bu<sub>2</sub> as a dark purple solid. The product was purified by Soxhlet extraction with methanol and hexanes to remove low molecular weight and inorganic impurities to yield a polymer that was fully soluble in THF, toluene, chloroform, and methylene chloride. The polymer has a <sup>1</sup>H NMR spectrum (Figure 1, top) that is consistent with the linear polymerization depicted in Scheme 1, with no end group signals evident. Notably, the polymer does react with deuterated chloroform, possibly through some form of doping, over time (ca. 6 h) as evidenced by unassignable <sup>1</sup>H NMR peak shapes and loss of visual fluorescence of the solution. This effect was eliminated using deuterated benzene as the NMR solvent, and as long acquisition times were needed for <sup>13</sup>C NMR (Figure 1, bottom), hydrazine was added to the solution to keep the polymer in the neutral state. Again, the expected peaks for the alkyl and thiophene carbons in the linear polymer are present.

**Molecular Weight Characterization.** The PProDOT-Bu<sub>2</sub> molecular weight was analyzed using both GPC and MALDI-TOF-MS. GPC yields chromatographs with peaks where there is severe "tailing", indicating a likely adsorption of the polymer to the columns which made quantitation of molecular weight distributions difficult. The *M<sub>p</sub>* value in THF relative to polystyrene was measured as 6000 g/mol for PProDOT-Bu<sub>2</sub>, which corresponds to an *X<sub>n</sub>* value of 22. It should be noted that while very high *X<sub>n</sub>* is not needed to obtain the electrical and optical properties that are desired, higher molecular weights may enhance polymer processing and film formation.

MALDI-TOF-MS was a useful tool in the structural characterization of PProDOT-Bu<sub>2</sub>, and the results using terthiophene as the matrix are displayed in Figure 2. No cationization salt (typically a silver(I) salt) was used for these polymers, as they were found to oxidize the

polymer, and PProDOT-Bu<sub>2</sub> forms stable pseudomolecular ions (*M* + *H*)<sup>+</sup> without cationization salts. The correct repeat unit mass difference (266 amu, see inset to Figure 2) is observed between the peaks. Because this polymer has been fractionated by solvent extraction, an accurate molecular weight distribution can be estimated from the MALDI spectrum, making the assumption that all of the chains are equally MS active, irrespective of molecular weight. Applying these assumptions to the MALDI analysis, PProDOT-Bu<sub>2</sub> has a *M<sub>n</sub>* value of 5400, *M<sub>w</sub>* of 5900, a polydispersity of 1.08, and an *X<sub>n</sub>* value of 20. A close examination of the MALDI spectrum shows there are three different distributions stemming from chains with three different types of end groups. The inset of Figure 2 shows an expanded set of MALDI peaks and exhibits how the functional group distribution was determined. The results are similar in nature to those reported by McCullough and co-workers for poly(3-alkylthiophene)s, where chains with three types of end groups were found.<sup>26</sup> Analysis reveals that the

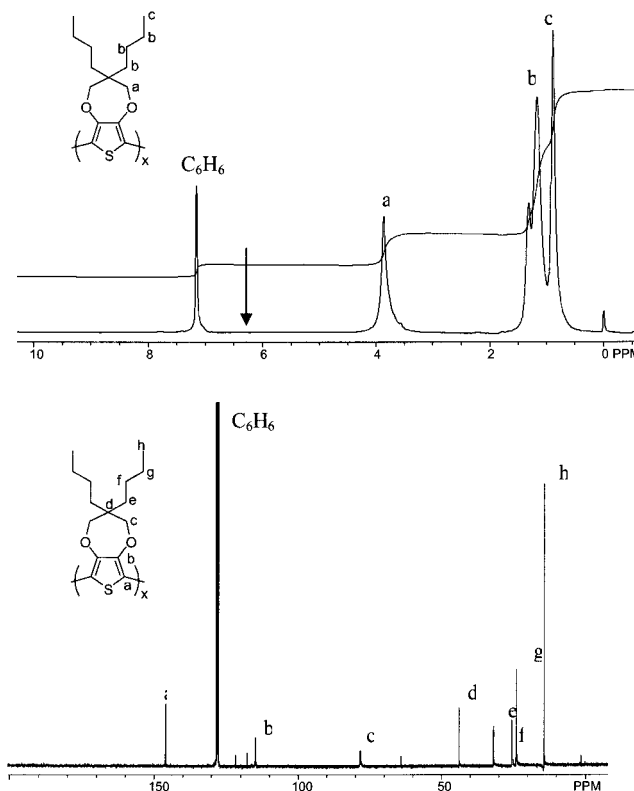


**Figure 1.** <sup>1</sup>H (top) and <sup>13</sup>C (bottom) NMR spectra of PProDOT-Bu<sub>2</sub> in C<sub>6</sub>D<sub>6</sub> with the chemical shifts and structures labeled. The arrow on the <sup>1</sup>H NMR spectrum shows where a 3,4-ethylenedioxythienyl end group proton resonance would be expected.

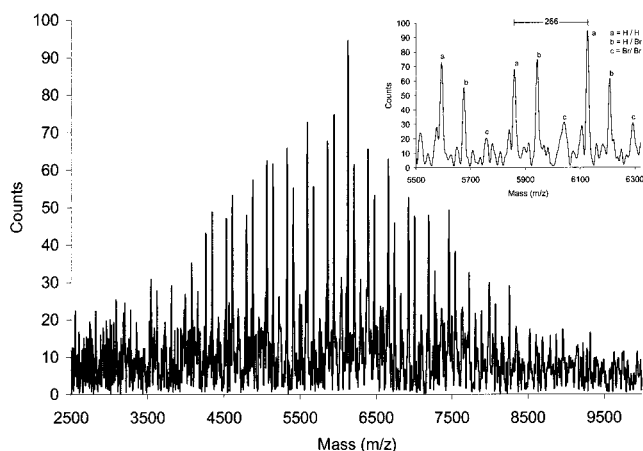


**Figure 2.** MALDI-TOF-MS of PProDOT-Bu<sub>2</sub> showing the full range of molecular weights accessible. The inset shows a close-up of the 5500–6300 *m/z* region with labels indicating the end groups present: (a) H/H, (b) H/Br, (c) Br/Br.

*m/z* of each peak can be represented by  $(266n + 1 + 1)$ ,  $(266n + 80 + 1 + 1)$ , and  $(266n + 80 + 80 + 1)$ , where *n* is equal to the number of repeat units. It should be noted that the resolution is insufficient to resolve the bromine isotopes. From these values, it can be concluded that the three types of end groups correspond to polymer chains that are terminated by two hydrogen atoms, one hydrogen atom and a bromine atom, and two bromine atoms. The McCullough group found that the relative abundance of these types of end groups are variable and depend on small changes in polymerization conditions that cannot be controlled easily.<sup>26</sup> The limitations of MALDI should be noted when considering the accuracy of these molecular weights, and even though the PDI value is less than 1.2, these numbers could still be biased low due to poor detection of higher molecular weight chains.

**Thermal Properties.** The thermal stability of neutral PProDOT-Bu<sub>2</sub> was studied by thermogravimetric analysis (TGA) in a nitrogen atmosphere using a temperature ramp from 50 to 800 °C at a rate of 20 °C/min. The thermogram shows that degradation onsets at 250 °C with a slow 8% weight loss prior to a major degradation process at 380 °C with approximately 27% of the material remaining at 800 °C. Differential scanning calorimetry (DSC) analysis showed no transitions in the temperature range from 25 to 300 °C.

**Electronic Spectroscopy.** The UV-vis spectra of PProDOT-Bu<sub>2</sub> in the solid state before and after an electrochemical oxidation and reduction cycle and in solution are shown in Figure 3. Solution cast (toluene, 2% w/w) vacuum-dried films of PProDOT-Bu<sub>2</sub> are reddish-purple and have a  $\lambda_{\text{max}}$  value of 544 nm, essentially identical to the  $\lambda_{\text{max}}$  observed in solution (542 nm). When the films are electrochemically oxidized and then subsequently reduced, their color changes to a dark purple color with a  $\lambda_{\text{max}}$  that is red-shifted to 576 nm. In addition, the absorption band exhibits better resolved fine structure. The latter spectrum is very similar to that of electrochemically polymerized and charge neutralized PProDOT derivatives.<sup>16</sup> The red-shifting and better resolved fine structure are attributed to a doping-induced ordering of the polymer in the solid state. The fine structure that is observed in the film absorption spectra may arise from vibronic coupling or, as discussed recently by Curtis and co-workers,<sup>27</sup> may be due to different absorption peaks arising from conjugated

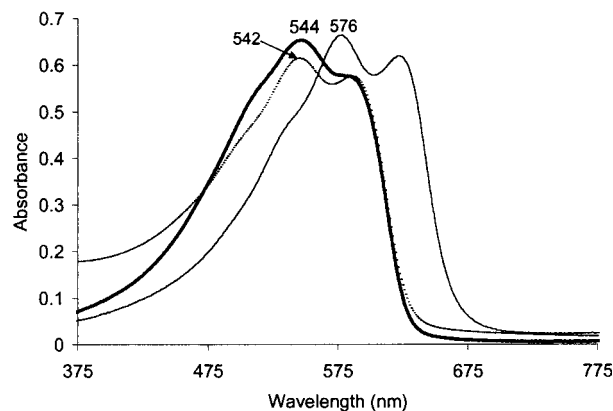


**Figure 3.** UV-vis spectrum of PProDOT-Bu<sub>2</sub> in CH<sub>2</sub>Cl<sub>2</sub> solution (dotted line,  $\lambda_{\text{max}}$  = 542 nm), in the solid state as cast from toluene (thick line,  $\lambda_{\text{max}}$  = 544 nm), and after electrochemical oxidation and reduction (thin line,  $\lambda_{\text{max}}$  = 576 nm).

segments having different conjugation lengths. A similar behavior was observed in solution for poly(3-octylthiophene) by Apperloo et al.,<sup>28</sup> where the authors attribute this to the partial quinoid geometry of the oxidized state, which reduces conformational disorder along the chain and causes preorganization of the chains. This preorganization is preserved upon dedoping and thus gives rise to the spectral changes. For comparison, the highest obtained  $\lambda_{\text{max}}$  for a regioregular head-to-tail poly(3-alkylthiophene) is 526 nm for thin films of poly(3-dodecylthiophene) (PDDT).<sup>7</sup> The red shift observed for PProDOT-Bu<sub>2</sub> is expected, because PProDOT-Bu<sub>2</sub> is significantly more electron-rich than PDDT, giving a raised HOMO level that reduces the band gap.

As seen in other conjugated polymers, the solution  $\lambda_{\text{max}}$  (542 nm) is blue-shifted (28 nm) when compared to the organized solid-state film, because the chains have more conformational freedom in solution, allowing for twisting of the thiophene rings out of plane. The shift from solid state to solution is much smaller in PProDOT-Bu<sub>2</sub> than PDDT, where  $\lambda_{\text{max}}$  of PDDT in solution is 450 nm, which is a 76 nm shift from the solid-state value.<sup>7</sup> This fact suggests that PProDOT-Bu<sub>2</sub> is either more ordered in solution than PDDT or less ordered in the solid state.

**Photophysics.** The photophysical properties of PProDOT-Bu<sub>2</sub> were characterized by variable temperature photoluminescence and microsecond laser flash photolysis spectroscopy. These experiments provide information concerning the singlet and triplet excited states that are produced by direct excitation of the polymer. Studies in solution were carried out in toluene and THF with essentially identical results. Consequently, only the toluene data are reported herein.

The fluorescence spectrum of PProDOT-Bu<sub>2</sub> in toluene is shown in Figure 4a along with the absorption of the polymer in the same solvent. The fluorescence band appears as a broad envelope consisting of three well-resolved vibronic bands, with a 0–0 transition at  $\lambda_{\text{max}}$  = 617 nm (2.0 eV). The spacing of the vibronic bands is approximately 1300 cm<sup>-1</sup>, which likely corresponds to C–C vibrational modes of the thiophene rings. The fluorescence of PProDOT-Bu<sub>2</sub> is red-shifted considerably from that of soluble poly(3-alkylthiophene)s,<sup>29</sup> consistent with the decreased band gap of PProDOT-Bu<sub>2</sub>. More interesting is the fact that the vibronic structure is much better resolved in PProDOT-Bu<sub>2</sub> compared to that of soluble poly(alkylthiophene)s.<sup>30</sup> In addition, the Stokes



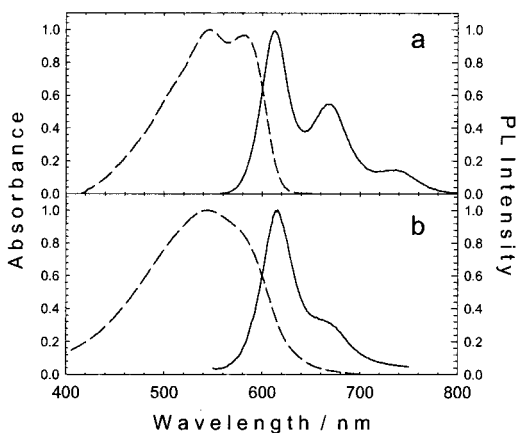


**Figure 4.** Normalized absorption (---) and photoluminescence (—) spectra of PProDOT-Bu<sub>2</sub>: (a) toluene solution,  $c = 5 \times 10^{-6}$  M ( $\epsilon$  is ca.  $15\,000\text{ M}^{-1}\text{ cm}^{-1}$ ); (b) drop cast film.

shift ( $\Delta = 1000\text{ cm}^{-1}$ ) is very low compared to that of poly(alkylthiophene)s (note the close proximity of the 0–0 absorption and fluorescence bands in Figure 4a).<sup>29,30</sup> Taken together, these features strongly suggest that PProDOT-Bu<sub>2</sub> has a more rigid structure compared to poly(alkylthiophene)s, possibly due to the fact that PProDOT-Bu<sub>2</sub> has a more planar (and consequently more delocalized) ground-state structure. In addition, the very small Stokes shift clearly indicates that there is little geometric change that occurs upon photoexcitation of the polymer.

Fluorescence quantum yields ( $\phi_f$ ) and decay lifetimes ( $\tau$ ) were determined for PProDOT-Bu<sub>2</sub> in toluene solution. The polymer fluoresces relatively efficiently, with  $\phi_f = 0.45$ . The fluorescence from PProDOT-Bu<sub>2</sub> in toluene solution decays via biexponential kinetics. The decay is dominated by a component having  $\tau = 720\text{ ps}$  (amplitude = 97%), but in addition a minor component with  $\tau = 7.1\text{ ns}$  (amplitude = 3%) is resolved. The fluorescence quantum yield and fluorescence decay kinetics of PProDOT-Bu<sub>2</sub> are very similar to those of regioregular poly(3-dodecylthiophene).<sup>31</sup> This correspondence indicates that the fluorescence properties of PProDOT-Bu<sub>2</sub> are similar to those of other structurally well-defined poly(thiophene)s.

A series of experiments were carried out to examine the absorption and fluorescence spectra of solid films of PProDOT-Bu<sub>2</sub>. These studies demonstrate that the band shape and wavelength maxima of the fluorescence and absorption spectra depend on the method used to cast the film (e.g., spin-coating or drop-casting). The spectra also varied from sample to sample. These observations indicate that the polymer's optical properties are dependent on the morphology of the solid. This is not surprising, since the conjugation length and interchain interactions are likely to vary with the polymer morphology.

Typical absorption and fluorescence spectra of a drop cast film of PProDOT-Bu<sub>2</sub> are shown in Figure 4b. The fluorescence from the cast film is considerably weaker than observed when the polymer is dissolved in solution, suggesting that interchain interactions in the solid lead to exciton quenching. Because of the difficulty of measuring fluorescence quantum yields on solids,<sup>32</sup> the fluorescence quantum yield of a PProDOT-Bu<sub>2</sub> film was not determined. However, on the basis of a qualitative comparison of the fluorescence intensity from PProDOT-Bu<sub>2</sub> films with that of films which are known to

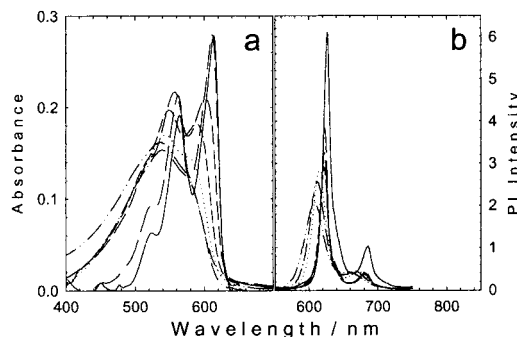


**Figure 5.** Variable temperature absorption and photoluminescence spectra of PProDOT-Bu<sub>2</sub> in 2-methyltetrahydrofuran solvent (glass). Spectra obtained at the following temperatures (listed in order of increasing intensity, lowest intensity first). (a) Absorption: 280, 220, 180, 140, and 90 K. (b) Fluorescence: 280, 220, 180, 140, 120, 90, and 77 K.

fluoresce efficiently, it is clear that the fluorescence quantum yield of PProDOT-Bu<sub>2</sub> films is very low. The fluorescence band is dominated by a strong 0–0 transition with a weak shoulder that is likely the 0–1 vibronic band. The shape of the spectrum is consistent with weak vibronic coupling, suggesting that the fluorescence in the solid arises from low-energy states that are localized on segments with a long conjugation length. The fluorescence decay of the cast film is dominated by a very short component with  $\tau = 190\text{ ps}$  (amplitude = 95%), and in addition a low-amplitude component with  $\tau = 5.3\text{ ns}$  (amplitude = 5%) is resolved. The very short lifetime observed for the solid polymer is consistent with the low emission yield and suggests that the decreased fluorescence yield is the result of rapid nonradiative decay at intrachain trap sites.

The absorption and fluorescence spectra of PProDOT-Bu<sub>2</sub> were measured in 2-MeTHF solution (glass) as a function of temperature over the range 77–280 K. As shown in Figure 5, with decreasing temperature the absorption spectrum red-shifts and develops vibronic structure, while the fluorescence intensity increases and the band red-shifts. At 77 K the absorption appears as a broad spectral envelope with three well-resolved vibronic bands with average spacing of  $1400\text{ cm}^{-1}$ . The red shift and increase in spectral resolution in the absorption spectrum that occurs with decreasing temperature signals an increase in conjugation length and structural ordering along the polymer backbone. This notion is supported by the fact that analogous red shifts with decreasing temperature have been observed for the absorption and fluorescence of poly(alkylthiophene)s, and in those systems the effect has been attributed to an increase in planarity of the ground-state polymer.<sup>29</sup> At low temperature the fluorescence appears as a set of very narrow vibronic bands with a bandwidth of  $\approx 250\text{ cm}^{-1}$  that are separated by  $1300\text{ cm}^{-1}$ . The increase in fluorescence intensity and band narrowing that occurs with decreasing temperature is expected, given the observed changes in the absorption spectrum. Non-radiative decay slows with decreasing temperature, accounting for the fluorescence intensity increase, while decreased coupling of the excited-state dipole with low-frequency solvent modes in the solvent glass at low temperature accounts for the narrowing of the vibronic bands.

Laser flash photolysis was carried out in order to probe for the existence of triplet excited states following direct excitation of PProDOT-Bu<sub>2</sub>. Pulsed excitation (532

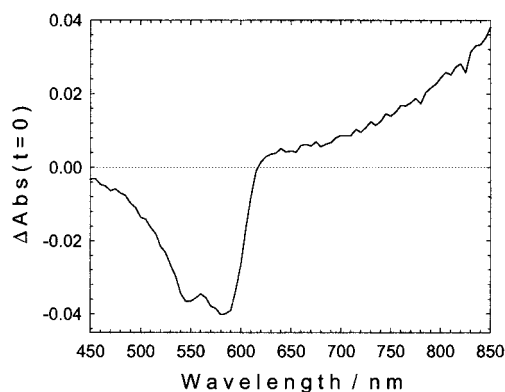


**Figure 6.** Principal component transient absorption difference spectrum obtained by 532 nm pulsed laser excitation of PProDOT-Bu<sub>2</sub> in argon-outgassed toluene solution. The spectrum is normalized on the  $\Delta A$  scale (y-axis) according to the transient absorption extrapolated to 0 delay time. The transient absorption decays with  $\tau = 25 \mu\text{s}$ .

nm) of a dilute solution ( $5 \times 10^{-6}$  M) of the polymer in toluene solution gives rise to a transient absorption that decays with a  $25 \mu\text{s}$  lifetime in argon-outgassed solution. On the basis of the lifetime and appearance of the spectrum (see below), we believe that this transient is the triplet excited state of the polymer. The triplet-state assignment is supported by the observation that the transient is very efficiently quenched by oxygen. The transient absorption difference spectrum, which is shown in Figure 6, is characterized by bleaching of the ground-state absorption band and transient absorption that increases throughout the red and extends into the near-IR. The rising transient absorption that appears in the red region of the spectrum suggests the onset of a band that has a maximum in the 900–1000 nm region (beyond the range accessible with our flash photolysis system). The appearance of the transient absorption difference spectrum is consistent with the triplet assignment. For example, the triplet excited state of poly(3-octylthiophene) features a strong absorption with  $\lambda_{\text{max}} \approx 850$  nm.<sup>33</sup> Given the fact that PProDOT-Bu<sub>2</sub> has a lower band gap compared to that of poly(3-octylthiophene), we anticipate that the triplet–triplet absorption of the former will be shifted to lower energy.<sup>34</sup> Although quantitative experiments were not carried out to determine the absolute absorptivity and yield of the PProDOT-Bu<sub>2</sub> triplet state, given the relatively low intensity of the transient absorption that is produced by direct excitation of the polymer, we estimate that the triplet yield is relatively low.

**Electrochemistry.** Cyclic voltammograms on glassy carbon for a solution cast film (toluene 2% w/w, thickness ca. 400 nm) of PProDOT-Bu<sub>2</sub> are compared to electrochemically prepared films in Figure 7. The latter film was prepared by potentiostatic polymerization at 1.3 V vs Ag/Ag<sup>+</sup> in order to produce a film of identical thickness. As expected for this electron-rich system, the switching potential is relatively low at about +0.2 V vs Ag/Ag<sup>+</sup>, which is lower than the value of +0.4 V vs Ag/Ag<sup>+</sup> observed for regioregular PDDT,<sup>35</sup> confirming the electron-rich nature of the PProDOT-Bu<sub>2</sub> system. The  $E_{1/2}$  values and general shape of the CV's are quite close to one another, showing that soluble polymers can be processed to provide films with similar characteristics as the electropolymerized versions. Upon repeated scanning after break-in up to 500 scans, there is a loss of 4% for the charge required to switch the solution cast

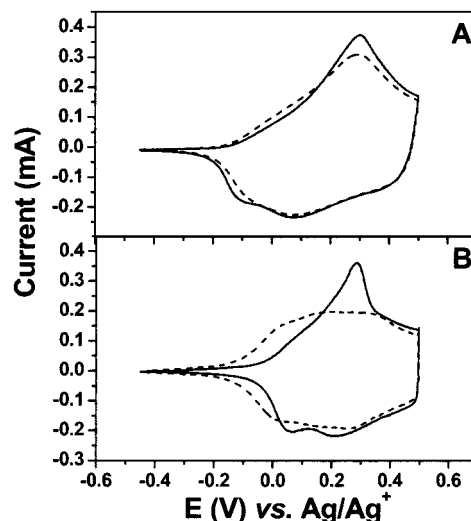


**Figure 7.** Cyclic voltammograms of PProDOT-Bu<sub>2</sub> on a glassy carbon working electrode for (A) a solution cast (toluene 2% w/w, thickness ca. 400 nm) film and (B) a potentiostatically deposited film (1.3 V vs Ag/Ag<sup>+</sup>, thickness ca. 400 nm) at 50 mV/s in 0.1 M TBAP/ACN. Scan numbers 20 (solid line) and 500 (dashed line) are presented.

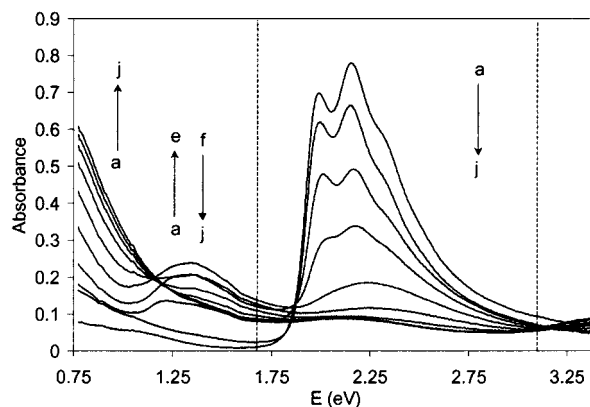


**Figure 8.** Spectroelectrochemistry of a solution cast film of PProDOT-Bu<sub>2</sub> in 0.1 M TBAP/ACN as a function of applied potential vs Ag/Ag<sup>+</sup>: (a) hydrazine reduced; (b)  $-1.0$ , (c)  $-0.2$ , (d)  $-0.1$ , (e)  $0.0$ , (f)  $+0.1$ , (g)  $+0.2$ , (h)  $+0.3$ , (i)  $+0.4$ , and (j)  $+0.5$  V.

film, while the electrochemically prepared film showed no change in the overall switching charge (though the peak current decreased and the response broadened). Both films exhibited a linear dependence of the peak currents with scan rates as expected for a non-diffusion-controlled redox response provided by a surface-attached electroactive material. As we did not observe delamination of the polymer from the electrode in either case, this loss of current, along with a broadening of the response in both cases, is attributed to reorganization of the chains (in essence an electrochemical annealing). These results are similar in nature to that observed<sup>16</sup> for PProDOT-Me<sub>2</sub> and are indicative of the long-lived electrochemical processes that are possible with this family of polymers.

**Spectroelectrochemistry and Electrochromic Switching.** A spectroelectrochemical series was obtained on a solution cast film (toluene, 2% w/w) of PProDOT-Bu<sub>2</sub> in 0.1 M tetrabutylammonium perchlorate (TBAP)/acetonitrile (ACN), and the results are displayed in Figure 8. When the polymer is held at a potential of  $-1.0$  V (Figure 8, curve b), there is a distinct

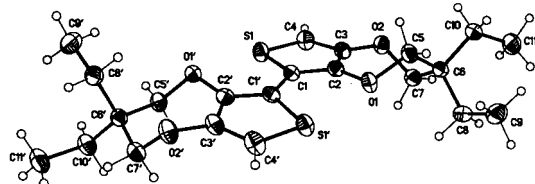


**Figure 9.** Perspective view and atom labeling of the crystal structure of BiProDOT-Et<sub>2</sub>.

$\pi$  to  $\pi^*$  transition with a band gap of 1.8 eV (689 nm) and two peaks at 2.0 eV (620 nm) and 2.2 eV (564 nm). These values are very close to those observed for the electrochemically synthesized PProDOT polymers previously published by us ( $E_g = 1.75$  eV).<sup>16</sup> Notice that there is a low-energy absorption tail; this is due to slight oxidation of the polymer and trapped charges. Upon addition of hydrazine to further reduce the polymer (Figure 6, curve a), the  $\pi$  to  $\pi^*$  transition increases in intensity, and the intensity of the low-energy tail decreases. Upon stepwise oxidation of the polymer, the  $\pi$  to  $\pi^*$  transition decreases and two lower energy transitions increase in intensity at 1.35 (918 nm) and below 0.75 eV (1653 nm). Similar to the electrochemically polymerized PProDOT's, the peak at 1.35 eV increases up to an applied potential of 0.0 V and subsequently decreases upon application of more anodic potentials. The fully oxidized form is reached by +0.5 V (recall this is near the  $E_{1/2}$  of PDDT) with only a low-energy NIR transition present. In this form, the low absorption throughout the visible region and lack of an absorption maximum causes the film to be very transmissive sky blue in color, again similar to the electrochemically synthesized films.

As discussed above with the photophysical results and the observed small Stokes shift for PProDOT-Bu<sub>2</sub>, the dihedral angle between the thiophene rings is an important factor in determining the electronic properties of a conjugated polymer. Previously, we have reported the synthesis of the 2,5-linked dimer of EDOT (BiEDOT) and shown through crystal structure data that the thiophene rings are coplanar with a torsional angle of 0° within experimental error.<sup>36</sup> To obtain the dihedral angle for the ProDOT-R<sub>2</sub> series, the dimer of PProDOT-Et<sub>2</sub> was synthesized by the lithiation and subsequent Fe(acac)<sub>3</sub> coupling of ProDOT-Et<sub>2</sub>, and its crystal structure is shown in Figure 9. The dihedral angle between the thiophene rings is 9.4°, quite close to planar, showing that there are no significant steric interactions between the thiophene rings. This is consistent with the spectroscopic results which imply that, in the ground state, the PProDOT-Bu<sub>2</sub> exists in a nearly planar conformation. An interesting feature of the crystal structure is the conformation of the propylenedioxy seven-membered rings. In the ring on the right side of the structure in Figure 9, the seven-membered ring is in a twist conformation, while the ring on the left is in a chairlike conformation. This shows that the seven-membered ring has sufficient conformational freedom to obtain the conformation to allow for planarity between the thiophene rings.

The spectroelectrochemical results demonstrate that the polymer film can be switched between the oxidized and reduced forms with an accompanying color change. To investigate the optical contrast and response times, solution cast and electrochemically prepared films of PProDOT-Bu<sub>2</sub> (400 nm) were switched by repeated double potential steps between reduced (-1.0 V) and

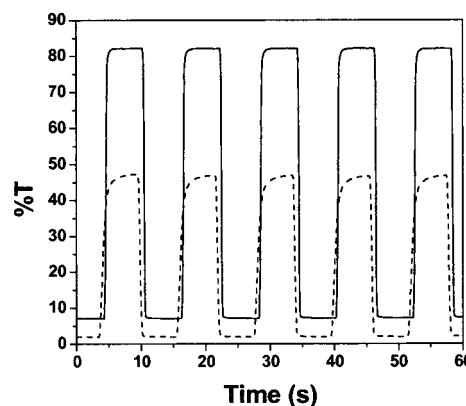


**Figure 10.** Electrochromic transmittance changes at  $\lambda_{\max}$  during repeated redox switching of PProDOT-Bu<sub>2</sub> (solid line, electrochemically prepared; dashed line, solution cast) between -1.0 and +0.8 V vs Ag/Ag<sup>+</sup> in 0.1 M TBAP/ACN with a step time of 6 s.

oxidized (+0.8 V) states while the transmittance changes at  $\lambda_{\max}$  were monitored. The results are displayed in Figure 10 for a switching time of 6 s, which allowed both films to be fully converted between states. It can be seen that the contrast is significantly higher for the electrochemically prepared film, suggesting that higher doping levels are achieved. While both films reduce quite rapidly and switch in less than 1 s, the oxidation is rapid for the electrochemically prepared film, yet slower for the solution cast film. This suggests that penetration of the dopant ion into the cast film is morphologically impeded. Holding either film for 60 s at each potential leads to little further change in their transmittance properties.

Analyzing the electrochemical and spectroscopic results, the main difference between solution cast films and electrochemically deposited films is morphology. Electrochemically polymerized films have an open morphology, while solution cast films tend to be more compact. This can hinder ion movement in and out of the film. These issues can be overcome by the preparation of multicomponent materials, e.g., polymer blends, where a highly ionic conductive (yet electroinactive) polymer is blended with the conducting polymer. For example, blends of poly(1,4-phenylenevinylene) (PPV) with polar carrier polymers can be electrochemically doped to high levels and at adequate rates where films of PPV alone are quite difficult to electrooxidize.<sup>37</sup>

The  $\Delta\%T$  value for a solution cast film (400 nm) of PProDOT-Bu<sub>2</sub> is about 45% (Figure 10), which is lower than that observed for electrochemically synthesized PProDOT-Bu<sub>2</sub> (75% for a 400 nm thick film). While both films oxidize to a more highly transmissive form, the solution cast reduced film is more absorptive than the electrochemically prepared film as one would expect for a more compact material. Although the electrochromic switching rates and contrast of the cast films are not quite as rapid as the electrochemically prepared films, the switching properties are quite high quality when compared to those presented for many other conducting polymers. The fact that the polymer is synthesized by a high yield solution polymerization is an immense benefit when compared to the low yields, usually leading to discarding of time intensively prepared monomer, obtained in electrochemical polymerizations.

**Solution Doping.** A further benefit of the solution polymerization methodology is that these polymers can



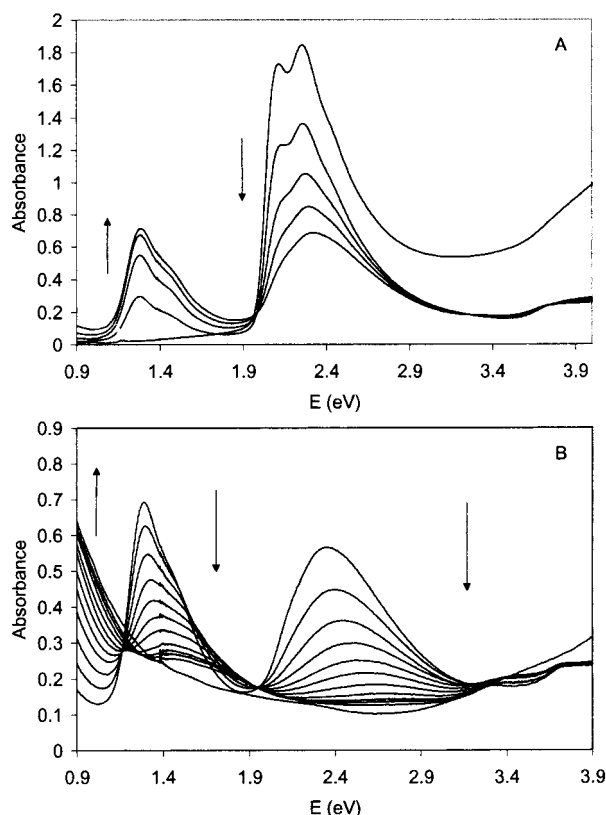


**Figure 11.** UV-vis-NIR spectra of a solution of PProDOT-Bu<sub>2</sub> in CH<sub>2</sub>Cl<sub>2</sub> as a function of addition of 2.0 uL aliquots of a 0.8 mM solution SbCl<sub>5</sub> in CH<sub>2</sub>Cl<sub>2</sub>. Part A displays initial doping, and part B displays final doping.

be converted into their oxidatively doped forms in solution, and the doped form can remain in solution for characterization and processing. This is demonstrated by the results of Figure 11, where a solution of PProDOT-Bu<sub>2</sub> in CH<sub>2</sub>Cl<sub>2</sub> was doped stepwise by addition of 2.0 uL aliquots of a 0.8 mM solution of SbCl<sub>5</sub> in CH<sub>2</sub>Cl<sub>2</sub>. The figure is divided into the initial (part A) and final (part B) doping steps for clarity. In Figure 11A, the neutral polymer solution shows a  $\pi$  to  $\pi^*$  transition with an onset of 1.95 eV (636 nm), peaks at 2.13 eV (582 nm) and 2.27 eV (546 nm), and the dilute reduced solution appears light purple in color. These results are in line with the results of Figure 4 shown for a toluene solution where the absorbance peaks are at 582 and 545 nm. Note that the spectrum with the highest intensity of the peak at 2.27 eV is reduced with hydrazine, which was required to attain the fully reduced form. Upon titration of the oxidant, the  $\pi$  to  $\pi^*$  transition decreases with the subsequent increase of a lower energy peak at 1.3 eV (954 nm) and an absorbance near 0.9 eV (1378 nm). Similar to the behavior of the film spectroelectrochemistry discussed earlier, at higher doping levels (Figure 11B) the peak at 1.3 eV decreases until only one transition is observed which would peak at wavelengths outside the limits of the spectrophotometer used. Again, there is very little absorption in the visible region, and the oxidized solution appears as a very transmissive light blue. The changes in the electronic transitions upon doping comply with the transitions calculated to be strongly allowed by Fesser, Campbell, and Bishop in the FBC theory.<sup>38</sup> At low doping levels, polarons are the main charge carriers giving rise to two lower energy transitions, while at high doping levels bipolarons are formed, giving rise to a lower energy transition below

0.9 eV. These results are very similar to those obtained by Apperloo et al. for poly(3-octylthiophene) doped in solution by thianthrenium perchlorate.<sup>39</sup> The authors attribute the highly transmissive oxidized form to the ability of thianthrenium perchlorate to dope the polythiophene to very high levels. At these high doping levels, polarons on the same chain are forced to combine into bipolarons, which leads to a bipolaron-rich material. Since the bipolaron-rich material exhibits only one peak well into the NIR, there is very little absorbance in the visible region, leading to a highly transmissive material. Following this argument, because PProDOT-Bu<sub>2</sub> exhibits a similar highly transmissive oxidized form in both solution and the solid state (see above), it is concluded that PProDOT-Bu<sub>2</sub> can be doped to very high levels with the weaker oxidant.

**Conductivity.** By increasing the amount of MeMgBr used in the polymerization to compensate for catalyst activation, a polymer of higher molecular weight was obtained as evidenced by the lack of complete solubility and lower bromine content in the elemental analysis. Upon removal of solvent during purification, the sample forms a reflective free-standing film which could not be fully dissolved. Four-point probe conductivities of the film of PProDOT-Bu<sub>2</sub> were measured on iodine-doped samples. Conductivities of 2 S/cm were measured and remained stable after the film was placed under vacuum for 24 h. The conductivity of the film increased to 7 S/cm after exposure to atmospheric conditions for 2 days and remained stable for over 1 month. After 4 months storage in the open laboratory (and at least one inadvertent instance where water was spilled on the sample), the conductivity remained high at 1.2 S/cm.

**Conclusions and Perspective.** Dioxythiophene-based polymers provide enhanced oxidative doping properties when compared to their P3AT counterparts due to the reduction in oxidation potential and band gap provided by the electron-donating substituents. Here, we have demonstrated that the GrIM polymerization method can be applied to the preparation of soluble poly(3,4-alkylenedioxythiophene)s. By utilizing the propylenedioxy bridge, disubstitution at the central carbon of the bridge affords symmetric monomers that polymerize to yield polymers having regiosymmetric structures. PProDOT-Bu<sub>2</sub> solutions are intensely photoluminescent and emit red light, with high quantum efficiencies. While this intense emission is substantially quenched in the solid state, this is likely due to enhanced nonradiative decay at trap sites arising from interactions between neighboring chains and suggests that polymers having larger and/or bulkier substituents will provide enhanced solid-state luminescence. The low redox potential allows solution cast films to be switched between the polymer's reduced and oxidized states easily. While the optical contrast is as desired for a cathodically coloring electrochromic material, the contrast ratios observed for solution cast films are lower than for those prepared by direct electrodeposition methods. The oxidized form of the polymer can remain in solution for sufficient times for it to be cast to form conducting films, and the highly conducting form of the polymer (ca. 5–10 S/cm) is quite stable when exposed to ambient atmosphere conditions.

## Experimental Section

**Materials.** 3,4-Dimethoxythiophene was synthesized as previously reported.<sup>40</sup> NBS was obtained from Acros and

recrystallized from water prior to use. Methylmagnesium bromide in butyl ether was purchased from Aldrich, and the exact molarity was determined by titration with a solution of 0.25 M 2-butanol and 0.005 M *N*-phenyl-1-naphthamine in *p*-xylene. TBAP was prepared by mixing a 1:1 mole ratio of tetrabutylammonium bromide (Aldrich) dissolved in water with perchloric acid. The precipitate was filtered, recrystallized from ethanol, and dried in vacuo. Acetonitrile (Aldrich) was dried over calcium hydride and distilled under argon. Toluene (Fisher) was dried over sodium metal and distilled under argon. Tetrahydrofuran (THF) was dried over NaK and distilled under argon. *p*-Toluenesulfonic acid and Ni(dppp)-Cl<sub>2</sub> were obtained from Aldrich and used as purchased. Chloroform was obtained from Fisher and used as purchased.

**Instrumentation.** NMR spectra were recorded on a Gemini 300 FT-NMR, a VXR 300 FT-NMR, or a Varian XL-300 FT-NMR. Mass spectrometry was carried out on a Finnigan MAT 95Q mass spectrometer. Elemental analyses were accomplished at Robertson Microlit Laboratories, Inc., Madison, NJ. FT-IR spectra of samples prepared as thin films on NaCl plates were obtained using a Perkin-Elmer 1640 FT-IR spectrometer.

GPC was performed on two 300 × 7.5 mm Polymer Laboratories PLGel 5uM mixed-C columns with a Waters Associates liquid chromatography 757 UV absorbance detector at 550 nm. Molecular weights were referenced to polystyrene standards (Polymer Laboratories). Polymer samples were prepared in THF (1 mg/mL) and passed through a 50uM filter prior to injection. A constant flow rate of 1 mL/min was used. MALDI-TOF-MS were obtained on a Bruker reflex II mass spectrometer equipped with delayed extraction (Bruker Daltonics, Manning Park, Billerica, MA). The accelerating voltage was 21 keV with a delay of 50 ns. The system was operated in reflectron mode. Both terthiophene and dithranol were used as matrices with better resolution in terthiophene. Samples were prepared from a 1:1 combination of a THF solution of 0.1 M terthiophene and 1 × 10<sup>-4</sup> M THF solution of polymer. This mixture was then spotted on the MALDI sample plate.

UV-vis-NIR spectra were recorded using a Varian Cary 5E UV-vis-NIR spectrophotometer. Fluorescence data were obtained with a Spex F-112 photon counting fluorimeter at room temperature. Emission quantum yields were measured relative to Rhodamine 6G in methanol at 1.00 × 10<sup>-6</sup> M where  $\phi_F = 1.00$ , and the optical density of the solutions was kept below  $A = 0.1$ . Thermogravimetric analysis was obtained with a Perkin-Elmer TGA 7 thermogravimetric analyzer. Differential scanning calorimetry (results not shown) was obtained on a Perkin-Elmer DSC 7 differential scanning calorimeter. Polymer electrochemistry was carried out on an EG&G Princeton Applied Research model 273A potentiostat/galvanostat with a glassy carbon button working electrode, a platinum flag counter electrode, and a Ag wire pseudo-reference electrode calibrated to the Ag/Ag<sup>+</sup> reference electrode (10 mM AgNO<sub>3</sub> in CH<sub>3</sub>CN) using ferrocene as an internal standard. Spectroelectrochemistry was performed using a Varian Cary 5E UV-vis-NIR spectrophotometer. A three-electrode cell was used with an ITO-coated glass slide (7 × 50 × 0.6 mm, 20 Ω/□ Delta Technologies) as the working electrode, a platinum wire counter electrode, and a Ag/Ag<sup>+</sup> reference electrode all contained in a normal UV-vis cuvette. Potentials were applied using the same EG&G potentiostat as described above. Polymer films were cast on both the platinum button and ITO slide with a micropipet from a 2% solution of polymer in toluene. The films were dried under a nitrogen blanket prior to use.

Laser flash photolysis was carried out on an instrument that has been previously described.<sup>41</sup> Excitation was effected by using the second harmonic output of a Nd:YAG laser (532 nm, 5 mJ pulse<sup>-1</sup>, 10 ns fwhm). Samples were contained in a recirculating flow cell with a total volume of 10 mL to minimize possible effects due to sample decomposition in the volume excited by the laser. The multiwavelength time-resolved transient absorption data set was analyzed by singular value decomposition (Factor analysis) using the SPECFIT32 program (Spectrum Software Associates, 2001) to extract the

principal component transient absorption spectrum and the transient absorption decay kinetics.

**Synthesis. 3,3-Dibutyl-3,4-dihydro-2H-thieno[3,4-*b*]-[1,4]dioxepine (ProDOT-Bu<sub>2</sub>) (1).** 5.0 g (0.035 mol) of 3,4-dimethoxythiophene, 6.86 g (0.036 mol) of 2,2-dibutyl-1,3-propanediol, 0.20 g of *p*-toluenesulfonic acid, and 200 mL of toluene were combined in a two-neck flask equipped with a Soxhlet extractor with type 4A molecular sieves in the thimble. The solution was heated to reflux and allowed to reflux for 1 day. The reaction mixture was cooled and washed with water. The toluene was removed under vacuum, and the crude product was purified by column chromatography on silica gel with 3:2 hexanes/methylene chloride as the eluent to yield 6.5 g (69%) of compound **1** as a colorless oil. <sup>1</sup>H NMR (CDCl<sub>3</sub>):  $\delta$  0.92 (t, 6H); 1.20–1.42 (m, 12H); 3.85 (s, 4H); 6.42 (s, 2H). <sup>13</sup>C NMR (CDCl<sub>3</sub>):  $\delta$  14.05, 23.53, 25.00, 31.53, 43.62, 77.53, 104.64, 149.68. MS (CI) exact mass calcd (m + 1): 269.1575. Found: 269.1572. Elemental Analysis: Calculated for C<sub>15</sub>H<sub>24</sub>O<sub>2</sub>S: C, 67.12; H, 9.01; S, 11.94. Found: C, 66.83; H, 9.00; S, 11.54.

**6,8-Dibromo-3,3-dibutyl-3,4-dihydro-2H-thieno[3,4-*b*]-[1,4]dioxepine (ProDOT-Bu<sub>2</sub>-Br<sub>2</sub>) (2).** 1 g (3.7 mmol) of compound **10c** was dissolved in 100 mL of chloroform in a two-neck flask equipped with an argon inlet. Argon was bubbled through the solution for 20 min, and then 2 g (11.1 mmol) of NBS was added. The clear yellow solution was stirred at room temperature for 4 h, after which the solution was a dark brownish-red color. The chloroform was removed under vacuum, and the resulting residue was purified using column chromatography on silica gel with 8:2 hexanes/methylene chloride as the eluent to yield (after two columns) 1.53 g (97%) of compound **2** as a clear viscous oil. <sup>1</sup>H NMR (CDCl<sub>3</sub>):  $\delta$  0.90 (t, 6H), 1.30 (m, 12H), 3.88 (s, 4H). <sup>13</sup>C NMR (CDCl<sub>3</sub>):  $\delta$  14.20, 23.52, 26.04, 31.88, 44.21, 78.14, 90.82, 147.29. Elemental Analysis: Calculated for C<sub>15</sub>H<sub>22</sub>Br<sub>2</sub>O<sub>2</sub>S: C, 42.27; H, 5.20; S, 7.52. Found: C, 42.47; H, 5.02; S, 7.84.

**Poly(3,3-dibutyl-3,4-dihydro-2H-thieno[3,4-*b*]-[1,4]dioxepine) (PProDOT-Bu<sub>2</sub>).** MeMgBr solution in butyl ether was titrated as described above, and the concentration was found to be 0.925 M. 0.400 g (0.939 mmol) of compound **2** was dissolved in 25 mL of freshly distilled THF. 1.02 mL (0.9 mmol) of MeMgBr in butyl ether was added, and the colorless solution was heated to reflux. After 1 h, 0.013 g (2 mol %) of Ni(dppp)-Cl<sub>2</sub> was added, and the bright red mixture was heated at reflux for 20 h. The polymer was precipitated into 200 mL of methanol and filtered into a Soxhlet thimble. Soxhlet extractions were performed for 24 h with methanol and 48 h with hexanes to remove impurities. A subsequent Soxhlet extraction with methylene chloride was used to dissolve the polymer from the thimble, and the methylene chloride was removed to yield a dark purple solid (0.15 g, 60%) of PProDOT-Bu<sub>2</sub>. <sup>1</sup>H NMR (CDCl<sub>3</sub>):  $\delta$  0.90 (bm, 6H), 1.20 (bm, 12H), 3.87 (bm, 4H). <sup>13</sup>C NMR (CDCl<sub>3</sub>):  $\delta$  13.10, 22.64, 24.14, 30.62, 42.51, 62.80, 77.05, 113.50, 116.42, 120.48, 144.69. IR (neat, cm<sup>-1</sup>): 2957, 2931, 2863, 1468, 1430, 1370, 1041. Elemental analysis: Calculated for a chain taking into account the bromine content found and assuming one bromine and one hydrogen as end groups: H-(C<sub>15</sub>H<sub>22</sub>O<sub>2</sub>S)<sub>31</sub>-Br: C, 66.97%; H, 8.26%; S, 11.92%; Br, 0.95%. Found: C, 65.86%; H, 8.23%; S, 11.61%; Br, 0.95%.

**Free-Standing Film Sample of PProDOT-Bu<sub>2</sub>.** Elemental analysis: Calculated for a chain taking into account the bromine content found and assuming one bromine and one hydrogen as end groups: H-(C<sub>15</sub>H<sub>22</sub>O<sub>2</sub>S)<sub>49</sub>-Br: C, 67.21%; H, 8.28%; S, 11.96%; Br, 0.61%. Found: C, 66.00%; H, 8.12%; S, 11.86%; Br, 0.61%.

**BiProDOT-Et<sub>2</sub>.** 0.5 g (2.3 mmol) of ProDOT-Et<sub>2</sub> and 0.53 g (4.6 mmol) of TMEDA was dissolved in 25 mL of THF, cooled to -78 °C where 1.16 mL (2.9 mmol) of 2.5 M <sup>*n*</sup>BuLi in hexanes was added, and the solution was stirred for 40 min. After raising the temperature to 0 °C, the solution was transferred via cannula to a refluxing solution of 0.81 g (2.3 mmol) of Fe(acac)<sub>3</sub> in 25 mL of THF, and the red solution was refluxed overnight. The THF was removed under vacuum, and the resulting red solid was run through a plug of silica gel with chloroform as the eluent to yield a green solid. The solid was



dissolved in chloroform and two drops of hydrazine hydrate was added, and the chloroform was removed under vacuum to yield 0.4 g (80%) of BiProDOT-Et<sub>2</sub> as a yellow solid; mp 121–123 °C. <sup>1</sup>H NMR (C<sub>6</sub>D<sub>6</sub>): δ 0.59 (t, 12H), 1.16 (q, 8H), 3.59 (s, 4H), 3.71 (s, 4H), 6.33 (s, 2H). <sup>13</sup>C NMR (CDCl<sub>3</sub>): δ 7.21, 23.65, 43.90, 77.09, 77.15, 102.82, 115.10, 145.05, 149.57. Elemental analysis: Calculated for C<sub>22</sub>H<sub>30</sub>O<sub>4</sub>S<sub>2</sub>: C, 62.53%; H, 7.16%; S, 15.17%. Found: C, 62.40%; H, 7.11%; S, 15.00%. HRMS calculated for C<sub>22</sub>H<sub>30</sub>O<sub>4</sub>S<sub>2</sub>: 422.1585. Found: 422.1588.

**X-ray Crystallography; Data Collection, Structure Solution, and Refinement.** Data were collected at 173 K on a Siemens SMART PLATFORM equipped with a CCD area detector and a graphite monochromator utilizing Mo K $\alpha$  radiation ( $\lambda$  = 0.710 73 Å). Cell parameters were refined using up to 8192 reflections. A hemisphere of data (1381 frames) was collected using the  $\omega$ -scan method (0.3° frame width). The first 50 frames were remeasured at the end of data collection to monitor instrument and crystal stability (maximum correction on I was <1%). Absorption corrections by integration were applied based on measured indexed crystal faces.

The structure was solved by the Direct Methods in *SHELXL5* and refined using full-matrix least squares. The non-H atoms were treated anisotropically, whereas the hydrogen atoms were calculated in ideal positions and were riding on their respective carbon atoms. The thiophene rings are planar and have a dihedral angle of 9.37(9)° between them. The S1 seven-membered ring adopts a twist conformation with C5 and C7 located at distances of 0.815(3) and −0.779(3) Å, respectively, of the plane of atoms C2, C3, O1, and O2; atom C6 lies within 2 $\sigma$  of the same plane. On the other hand, the S1' seven-membered ring adopts a chair conformation where atoms C5', C6', and C7' are located at distances of −1.126(3), −1.046(3), and −1.133(3) Å, respectively, from the plane of C2', C3', O1', and O4'. A total of 257 parameters were refined in the final cycle of refinement using 4477 reflections with  $I > 2\sigma(I)$  to yield  $R_1$  and  $wR_2$  of 3.02% and 7.18 %, respectively. Refinement was done using  $F^2$ .<sup>42</sup>

**Acknowledgment.** We gratefully acknowledge support from the AFOSR (F49620-00-1-0047), the DARPA (DAAD 19-00-1-002), and the Xerox Corporation. K.A.A. acknowledges the NSF and the University of Florida for funding of the purchase of the X-ray equipment.

**Supporting Information Available:** Tables of crystallographic data for BiProDOT-Et<sub>2</sub>. This material is available free of charge via the Internet at <http://pubs.acs.org>.

## References and Notes

- (1) *Handbook of Conducting Polymers*, 2nd ed.; Skotheim, T. A., Elsenbaumer, R. L., Reynolds, J. R., Eds.; Marcel Dekker: New York, 1998.
- (2) Jen, K. Y.; Oboodi, R.; Elsenbaumer, R. L. *Polym. Mater. Sci. Eng.* **1985**, *53*, 79.
- (3) Elsenbaumer, R. L.; Jen, K. Y.; Oboodi, R. *Synth. Met.* **1986**, *15*, 169.
- (4) Miller, G. G.; Elsenbaumer, R. L. *J. Chem. Soc., Chem. Commun.* **1986**, 1346.
- (5) McCullough, R. D. *Adv. Mater.* **1998**, *10*, 93.
- (6) McCullough, R. D.; Lowe, R. D. *J. Chem. Soc., Chem. Commun.* **1992**, 70.
- (7) McCullough, R. D.; Lowe, R. D.; Jayaraman, M.; Anderson, D. L. *J. Org. Chem.* **1993**, *58*, 904.
- (8) Chen, T.-A.; Rieke, R. D. *Synth. Met.* **1993**, *69*, 175.
- (9) Chen, T.-A.; O'Brien, R. A.; Rieke, R. D. *Macromolecules* **1993**, *26*, 3462.
- (10) McCullough, R. D.; Tristram-Nagle, S.; Williams, S. P.; Lowe, R. D.; Jayaraman, M. *J. Am. Chem. Soc.* **1993**, *115*, 4910.
- (11) Groenendaal, L.; Jonas, F.; Freitag, D.; Pielartzik, H.; Reynolds, J. R. *Adv. Mater.* **2000**, *12*, 481.
- (12) Dietrich, M.; Heinze, J.; Heywang, G.; Jonas, F. *J. Electroanal. Chem.* **1994**, *369*, 87.
- (13) Heywang, G.; Jonas, F. *Adv. Mater.* **1992**, *4*, 116.
- (14) Sankaran, B.; Reynolds, J. R. *Macromolecules* **1997**, *30*, 2582.
- (15) Kumar, A.; Welsh, D. M.; Morvant, M. C.; Piroux, F.; Abboud, K. A.; Reynolds, J. R. *Chem. Mater.* **1998**, *10*, 896.
- (16) Welsh, D. M.; Kumar, A.; Meijer, E. W.; Reynolds, J. R. *Adv. Mater.* **1999**, *11*, 1379.
- (17) Sapp, S. A.; Sotzing, G. A.; Reynolds, J. R. *Chem. Mater.* **1998**, *10*, 2101.
- (18) Schwendeman, I.; Hwang, J.; Welsh, D. M.; Tanner, D. B.; Reynolds, J. R. *Adv. Mater.* **2001**, *13*, 634.
- (19) Kumar, A.; Reynolds, J. R. *Macromolecules* **1996**, *29*, 7629.
- (20) Schottland, P.; Fichet, O.; Teyssie, D.; Chevrot, C. *Synth. Met.* **1999**, *101*, 7.
- (21) Yamamoto, T.; Abila, M. *Synth. Met.* **1999**, *100*, 237.
- (22) Shiraishi, K.; Kanbara, T.; Yamamoto, T.; Groenendaal, L. B. *Polymer* **2001**, *42*, 7229.
- (23) Loewe, R. S.; Khersonsky, S. M.; McCullough, R. D. *Adv. Mater.* **1999**, *11*, 250.
- (24) Loewe, R. S.; Ewbank, P. C.; Liu, J.; Zhai, L.; McCullough, R. D. *Macromolecules* **2001**, *34*, 4324.
- (25) Wang, F.; Wilson, M. S.; Rauh, R. D.; Schottland, P.; Thompson, B. C.; Reynolds, J. R. *Macromolecules* **2000**, *33*, 2083.
- (26) Liu, J.; Loewe, R. S.; McCullough, R. D. *Macromolecules* **1999**, *32*, 5777.
- (27) Politis, J. K.; Nemes, J. C.; Curtis, M. D. *J. Am. Chem. Soc.* **2001**, *123*, 2537.
- (28) Apperloo, J. J.; Janssen, R. A. J.; Nielsen, M. M.; Bechgaard, K. *Adv. Mater.* **2000**, *12*, 1594.
- (29) Kang, T. J.; Kim, J. Y.; Kim, K. J.; Lee, C.; Rhee, S. B. *Synth. Met.* **1995**, *69*, 377.
- (30) Belletete, M.; Mazerolle, L.; Desrosiers, N.; Leclerc, M.; Durocher, G. *Macromolecules* **1995**, *28*, 8587.
- (31) Rumbles, G.; Samuel, I. D. W.; Magnani, L.; Murray, K. A.; DeMello, A. J.; Crystall, B.; Moratti, S. C.; Stone, B. M.; Holmes, A. B.; Friend, R. H. *Synth. Met.* **1996**, *76*, 47.
- (32) Greenham, N. S.; Samuel, I. D. W.; Hayes, G. R.; Phillips, R. T.; Kessener, Y.; Moratti, S. C.; Holmes, A. B.; Friend, R. H. *Chem. Phys. Lett.* **1995**, *241*, 89.
- (33) Matsumoto, K.; Fujitsuka, M.; Sato, T.; Onodera, S.; Ito, O. *J. Phys. Chem. B* **2000**, *104*, 11632.
- (34) Grebner, D.; Helbig, M.; Rentsch, S. *J. Phys. Chem.* **1995**, *99*, 16991.
- (35) McCullough, R. D.; Tristram-Nagle, S.; Williams, S. P.; Lowe, R. S.; Jayaraman, M. *J. Am. Chem. Soc.* **1993**, *115*, 4910.
- (36) Sotzing, G. A.; Reynolds, J. R.; Steel, P. J. *Adv. Mater.* **1997**, *9*, 795.
- (37) Schlenoff, J. B.; Machado, J. M.; Glatkowski, P. J.; Karasz, F. E. *J. Polym. Sci., Polym. Phys.* **1988**, *26*, 2247.
- (38) Fesser, K.; Bishop, A. R.; Campbell, D. K. *Phys. Rev. B* **1983**, *27*, 4804.
- (39) Apperloo, J. J.; van Haare, J. A. E. H.; Janssen, R. A. J. *Synth. Met.* **1999**, *101*, 417.
- (40) Gronowitz, S. *Ark. Kemi* **1958**, *12*, 239.
- (41) Wang, Y. S.; Schanze, K. S. *Chem. Phys.* **1993**, *176*, 305.
- (42) Sheldrick, G. M. *SHELXL5*; Bruker-AXS: Madison, WI, 1998.

MA0120409